doi: 10.3969/j.issn.0490-6756.2018.03.026

W 掺杂和电化学表面处理制备高光电化学性能的 $BiVO_4$ 光阳极

万丽娟[1,2], 杨　明[3]
(1. 南京交通职业技术学院, 南京 211188; 2. 江苏省交通节能减排工程技术研究中心, 南京 211188;
3. 东南大学交通学院, 南京 210096)

摘　要: 通过滴涂的方法合成了 W 掺杂 $BiVO_4$ 光阳极. 通过 XRD、紫外—可见吸收光谱、扫描电镜(SEM)对 $BiVO_4$ 光阳极进行表征,并对 $BiVO_4$ 光阳极进行了光电化学表征. 为了提高 W 掺杂 $BiVO_4$ 光阳极的光电性能,对 W 掺杂 $BiVO_4$ 光阳极的制备条件进行了优化. 光电化学测试结果表明电化学表面处理能够提高 W 掺杂 $BiVO_4$ 光阳极的光电化学性能. 说明 W 掺杂和电化学表面处理可以增加 $BiVO_4$ 光阳极光电流. 并进行了 $BiVO_4$ 光阳极光电流增加的机理分析.

关键词: $BiVO_4$; W 掺杂; 光阳极
中图分类号: O643.3　　**文献标识码**: A　　**文章编号**: 0490-6756(2018)03-0571-08

Synthesis of $BiVO_4$ photoanode with improved photoelectrochemical performance by W-doping and surface electrochemical pretreatment

WAN Li-Juan[1,2], *YANG Ming*[3]
(1. Nanjing Vocational Institute of Transport Technology, Nanjing 211188, China; 2. Jiangsu Engineering Technology Research Center for Energy Conservation and Emission Reduction of Transportation, Nanjing 211188, China;
3. School of Transportation, Southeast University, Nanjing 210096, China)

Abstract: W-doped $BiVO_4$ photoanode was obtained through drop-casting method. The physical and photophysical properties of the $BiVO_4$ photoanode were investigated by X-ray diffraction (XRD), UV-vis absorption spectroscopy and scanning electron microscopy (SEM). Photo-electrochemical performance was evaluated for the W-doped $BiVO_4$ photoanode. In terms of maximizing the photoelectrochemical performances of the W-doped $BiVO_4$ photoanodes, the synthesis conditions were optimized. The W-doped $BiVO_4$ photoanode exhibits improved photoelectrochemical performance after the electrochemical surface pretreatment. The photoelctrochemical response of $BiVO_4$ photoanode can be improved by both tungsten doping and the electrochemical surface pretreatment. A possible mechanism was also proposed to explain the reason for the photocurrent enhancement.

Keywords: $BiVO_4$; W-doped; Photoanode

收稿日期: 2017-01-04
基金项目: 南京交通联业技术学院科研基金(JZ1704); 江苏省高校自然科学研究面上项目基金(16KJD610004); 国家自然科学基金(51208102);南京交通职业技术学院高层次人才科研启动基金
作者简介: 万丽娟(1978－), 女, 山东章丘人, 助理研究员, 博士, 研究方向为环境科学. E-mail: bartty_ym@163.com

1 Introduction

Photocatalysis technique has a promising application for water splitting for hydrogen generation, removal of contamination [1] and *etc*. Photoelectrochemical splitting water for hydrogen production by utilizing solar energy represents a clean and renewable strategy to solve future energy challenges. However, to apply this technology, a photoelectrode should have characters of low cost, high quantum efficiency, narrow band gap and good photochemical stability. Some simple oxides with narrower band gaps due to their visible light response and fairly good stability, such as WO_3 and Fe_2O_3, have been studied intensively as photoelectrode materials [2,3]. In comparison with simple oxides, multi-metal oxides have more possibilities to adjust the chemical stability and electronic structure[4]. Among the systems explored to date, as a multi-metal oxide photoanode, monoclinic $BiVO_4$ (band gap ~ 2.4 eV) has received high expectations and become the most promising photoanode material candidate with high photoelectrochemical (PEC) performances in theory[5,6]. $BiVO_4$ which was suggested by Kudo *et al*. in 1998 as visible light-driven semiconductor, exhibited high activities for water oxidation[7]. $BiVO_4$ as photoanode material with its composition of earth abundant elements has the advantages of the efficient light absorption due to a relatively small band gap, and the oxidation of water to form O_2 (OER) due to the sufficiently positive valence band edge and *etc*[8,9]. However, due to the poor electron and hole mobility, inefficient interfacial charge separation, the retarded OER kinetics and *etc*., the water-splitting activity for bare $BiVO_4$ photoanode is quite low[10,11].

Among the methods to optimize the PEC performances, doping with ions is one desirable approach to resolve extensive carrier accumulation and recombination due to poor carrier transport properties. For $BiVO_4$, the carrier concentration is often increased by nonisovalent substitutional doping[4]. Various ions (Mo^{6+}, W^{6+}, Si^{4+}, Ti^{4+}, Ta^{5+}, Zr^{4+}, Fe^{3+}, La^{3+}, Zn^{2+}, Sr^{2+} and Ag^{+}) have been doped into the sites of V of $BiVO_4$ to improve the PEC performance and investigate the effects of nonisovalent substitutional doping, and only doping with Mo^{6+} or W^{6+} can obviously bring the most noticeable enhancement in the photocurrent[12]. Therefore, doping with tungsten can promote the increase of carrier concentration and the separation of photo-generated carriers[13], and the photoelectrochemical performances of $BiVO_4$ photoelectrodes doped with tungsten may be improved by optimizing the doping concentration and *etc*.

A suitable preparation method is also crucial for a photoelectrode material to realize the high PEC performance. On account of the application in a large scale and high PEC performance, the preparation method should be cheap, simple and easy to dope. Up to now, various methods have been used to prepare $BiVO_4$ photoelectrodes, such as metal-organic decomposition method[14], chemical bath deposition (CBD)[15], powder spreading[5,16], (ultrasonic spray pyrolysis) USP[13], electrodeposition[17], reactive ballistic deposition[18,19], drop-casting method [20] and *etc*. Among the synthesis methods, drop-casting method which eases doping is a facile method to prepare $BiVO_4$ photoelectrodes with good crystallinity, smaller grain size and high PEC performance.

To improve the photoelectrochemical performance of photoelectrodes, the surface modification of cocatalysts, such as Pt, Co_3O_4, Co-Pi, and RhO_2, is another desirable approach[4,20,21]. Recently, the surface pretreatment by electrochemical cyclic voltammetry (CV) in the dark as a simple pretreatment process has been reported to remove the surface recombination center of the Mo-doped $BiVO_4$, which is also expected as a universal way to increase the photoelectrochemical performances of the photoelectrode[22]. However, to the best of our knowledge, there has been no report regarding the improvement of the photocurrent of $BiVO_4$ photoanode by both W-doping and the electrochemical surface pretreatment. In

the present study, W-doped $BiVO_4$ photoanode was prepared via drop-casting method. With changing preparation conditions, the photoelectrochemical performances of the W-doped $BiVO_4$ photoanodes were analyzed. The preparation conditions were optimized in terms of maximizing the photoelectrochemical performances of the $BiVO_4$ photoanodes. The W-doped $BiVO_4$ photoanode exhibits improved photoelectrochemical performance after the electrochemical surface pretreatment and the possible mechanism was also discussed.

2 Experimental

2.1 Materials

The starting materials utilized are Bi_2O_3, NH_4VO_3, $(NH_4)_{10}W_{12}O_{41} \cdot 5H_2O$, ethylene glycol and nitric acid (analysis purity grade, Sinopharm Chemical Reagent Co. Ltd.).

2.2 Synthesis of W-doped $BiVO_4$ photoanode

W-doped $BiVO_4$ photoelectrodes were synthesized by drop-casting method. This sol-gel synthesis technique is simple, scalable and reproducible. Bi_2O_3, NH_4VO_3 and $(NH_4)_{10}W_{12}O_{41} \cdot 5H_2O$ were dissolved in ethylene glycol with proper amount of nitric acid to form 0.1 M Bi, V and W precursor solution respectively. Proper amount of these solutions were mixed according to the stoichiometric ratio. 70 μl of the precursor solution were dropped on the FTO (SnO_2: F on glass) substrates (2 cm × 1 cm). The samples were dried in a hot plate at 120 ℃ for 25 minutes and subsequently calcined at different temperatures in a tube furnace for a certain period of time. A pure $BiVO_4$ thin film was prepared by the same process as the reference.

2.3 Characterization

The products were characterized by X-ray diffraction (XRD) for phase identification on a Rigaku Ultima III diffractometer with Cu $K\alpha$ radiation (λ = 0.154 nm, 40 kV, 40 mA) and a scan rate of 10 ° · min^{-1}. Ultraviolet visible (UV-vis) transmission spectra were measured with a Varian Cary 50 spectrophotometer and the absorption spectra were obtained using the Kubelka - Munk method. The microstructure of the sample was observed by scanning electron microscopy (SEM) Philips XL30 with an electron accelerating voltage of 5 kV.

2.4 Photoelectrochemical (PEC) measurements

The photoelectrochemical properties were characterized by linear scanning voltammetry (LSV) technique performed on a CHI633C electrochemical workstation system. The LSV measurements were performed in a 0.5 M Na_2SO_4 aqueous solution (pH = 6.5) from −0.20 to 1.10 V with a scan rate of 20 mV · s^{-1} in a standard three-electrode configuration coupled with the sample films (working electrode), an Ag/AgCl electrode (reference electrode) and a high purity platinum (counter electrode). Before photoelectrochemical properties of the samples were measured, the pretreatment was carried out as follows [22]. The sample was scanned by cyclic voltammetry for 30 cycles in the electrolyte in the dark. The cyclic voltammetry scans were performed at the scan speed of 30 mV · s^{-1} and with threshold reduction potential (−0.9 V). The sample without surface electrochemical pretreatment was the reference. For photoelectrochemical measurement, an AM 1.5 G sunlight simulator (Oriel 92251A-1000) was used as a light source. The samples were illuminated from the front side (electrolyte/semiconductor interface). The mask-off irradiated area was 0.28 cm^2.

An AM 1.5 G sunlight simulator (Oriel 92251A-1000) was used as the light source to test the photostability of the W-doped $BiVO_4$ electrode. The light was illuminated from the front side of the $BiVO_4$ film photoelectrode. 0.5 M Na_2SO_4 aqueous solution (pH = 6.5) was used as the electrolyte. The electrode potential was 0.65 V vs. Ag/AgCl. The samples before and after illumination were investigated by XRD.

3 Results and discussion

The XRD patterns of the pure $BiVO_4$ and W-doped $BiVO_4$ films are shown in Fig. 1. The XRD

patterns indicate that all peaks in the $BiVO_4$ samples agree well with the characteristic pattern arising from a sheelite monoclinic structure (JCPDS No. 14-0688). The XRD pattern characteristic of WO_3 was not observed in W-doped $BiVO_4$ film, and no noticeable peaks appeared from any secondary phases such as Bi_2O_3, V_2O_5 in the XRD patterns, suggesting that tungsten was probably incorporated with $BiVO_4$. Furthermore, it is noteworthy that all peaks of W-doped sample has a slightly monotonically shift to low angel direction. The shifts have been assumed to be caused by the difference ion radii of W^{6+} and V^{5+} in the solid solutions which can slightly increase the crystal lattice[13] since it has been reported that the dopants occupy the V sites by using X-ray absorption spectroscopy[23]. Crystal deformation might be caused by a substitutional defect of V^{5+} ions being replaced by W^{6+}, which has larger tetrahedral ionic radii than V^{5+} (tetrahedral ionic radii for V^{5+} and W^{6+} are 0.35 and 0.42 Å, respectively)[24]. From Fig. 1, the peaks at 34.5° and 35.2° are indexed to the (200) and (002) lattices of the monoclinic scheelite-like $BiVO_4$ and the two peaks shift toward each other upon addition of W to the synthesis. Similar behavior is also observed for the peaks at 46.7° and 47.3° which are indexed to the (240) and (042) lattices of the monoclinic scheelite-like $BiVO_4$ upon addition of W to the synthesis. Similar shifts have been reported previously to arise from W doping in $BiVO_4$[10, 21].

The optical absorption of the pure $BiVO_4$ and W-doped $BiVO_4$ films samples was investigated using UV - vis absorption spectroscopy and shown in Fig. 2. The $BiVO_4$ films possessed a scheelite-monoclinic structure with good absorption to visible light. It has been reported that for $BiVO_4$, the conduction band minimum and valence band maximum consists of V-3d and the hybridization between the Bi-6s and O-2p orbitals respectively and the visible light absorption is relative to the Bi-6s electron lone pairs[12]. Compared with the pure $BiVO_4$ sample, the W-doped $BiVO_4$ sample shows blue shift to shorter wavelength. The absorption edge of the pure $BiVO_4$ and W-doped $BiVO_4$ sample occurs at ca. 500 and 492 nm, and the optical band gaps are evaluated to be about 2.48 and 2.52 eV respectively.

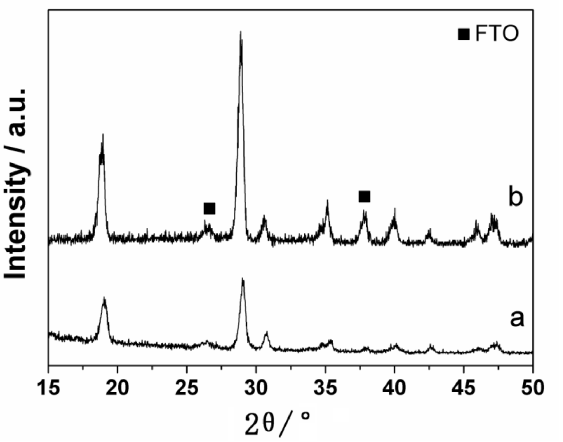

Fig. 1 XRD pattern of pure $BiVO_4$ film (a) and 2% W-doped $BiVO_4$ film (b) calcined at 500 ℃ for 30 min, (■) FTO substrates

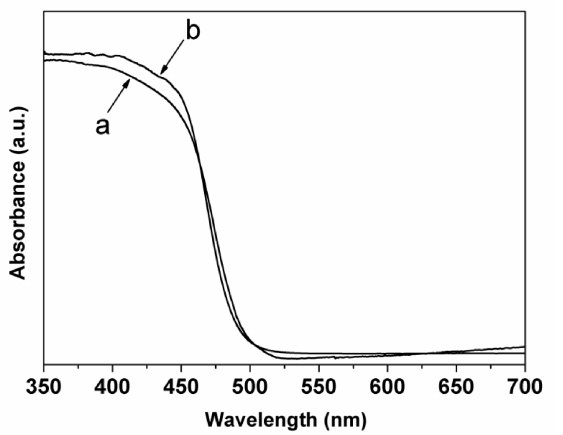

Fig. 2 The UV-vis absorption spectra of the pure $BiVO_4$ (a) and W-doped $BiVO_4$ (b)

SEM image of the W-doped $BiVO_4$ film prepared by drop-casting method is shown in Fig. 3. Porous structures consisting of particles with sizes of 100 - 500 nm are observed by SEM on the surface of the W-doped $BiVO_4$ film. The porous structures can allow the electrolyte to easily diffuse within the $BiVO_4$ network, increasing the contact area between the electrolyte and the photoanodes, and shortening the hole diffusion distance[2,3].

The photocurrent curves of W-doped $BiVO_4$ before

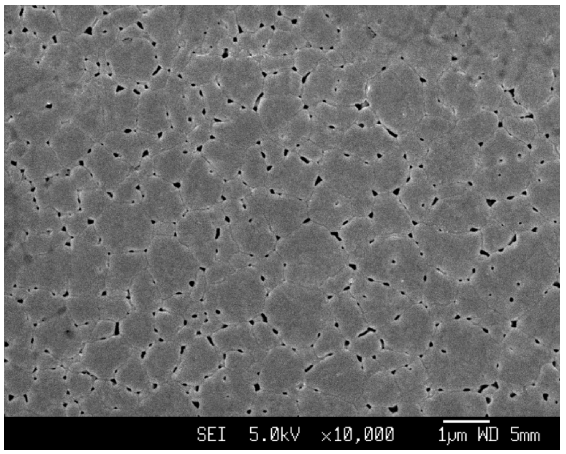

Fig. 3　SEM image of the surface of W-doped $BiVO_4$ film

and after surface pretreatment samples are shown in Fig. 4. The result shows that compared with the W-doped $BiVO_4$ sample without electrochemical pretreatment, the sample after the pretreatment shows the obvious enhancement of photocurrent. The pretreatment make the photocurrent of W-doped $BiVO_4$ sample at 0.9 V *vs.* Ag/AgCl three times more than that of the sample without pretreatment. It has been reported previously that the pretreatment can make some metal ions on the surface become reduced and others dissolved into the electrolyte and the photocurrent enhancement is mainly attributed to the dissolution of doping ions, which can be kept at high potential[22]. From the above results, it is proven that the electrochemical pretreatment is also a efficient method to improve the photocurrent of the W-doped $BiVO_4$ sample for the removal of surface recombination center.

Through optimizing the doping concentration or other preparation conditions, the photocurrent of W-doped $BiVO_4$ photoelectrodes may be improved. After the surface pretreatment, the $BiVO_4$ samples prepared at different conditions are investigated. The photocurrent curves of the pure and W-doped $BiVO_4$ samples with different doping concentrations are shown in Fig. 5. Compared with the pure $BiVO_4$ film, the photocurrent of the doped film shows a significant increase. The improved photoelectrochemical performance may come from the extending electron lifetime by dramatically altering the nature of the trap states for the reduced dimension and less distorted local structure at Bi center[23]. The result shows that the photocurrent is obviously improved at potential higher than 0.5 V when the doping concentration is increased from 1 % to 2 %. At potential of 1.0 V, the photocurrent of the W-doped $BiVO_4$ is increases to 1.2 times after the doping concentration is increased from 1 % to 2 %. The increase of the photocurrent may be contributed to the improved conductivity and quite different surface properties induced by tungsten doping. Doping with tungsten can also promote the separation of photo-generated carriers which can improve the photocurrent[13]. While for the sample with the doping concentration of 3 %, the photocurrent is lower than those with the doping concentration of 1 % or 2 %. That indicates that higher doping concentration may induce the increase of the recombination of photo-generated carriers and thus decrease the photocurrent because the dopant can also form recombination sites for photo-induced carriers [13]. Furthermore, doping can raise issues that counteract the enhanced carrier transport, for example, the incorporation of dopants can introduce trap states usually serving as recombination centers and then hinder interfacial charge separation[22]; doping can also decrease the width of the depletion layer and thus enhance carrier recombination and decrease the photocurrent[25].

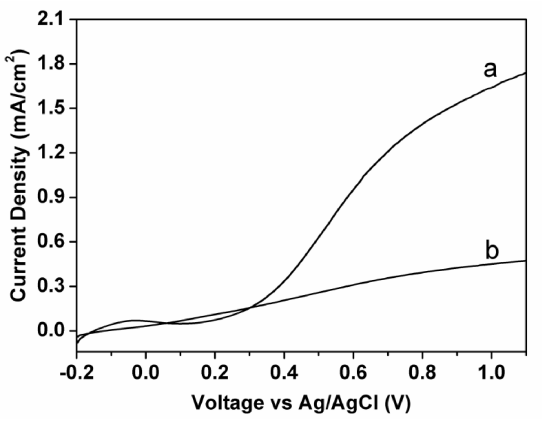

Fig. 4　Photocurrent curves of the $BiVO_4$ sample by 2 % W-doped and calcined at 500 ℃ for 30 min. a. After surface pretreatment; b. Before surface pretreatment

The influence of calcination temperatures on the

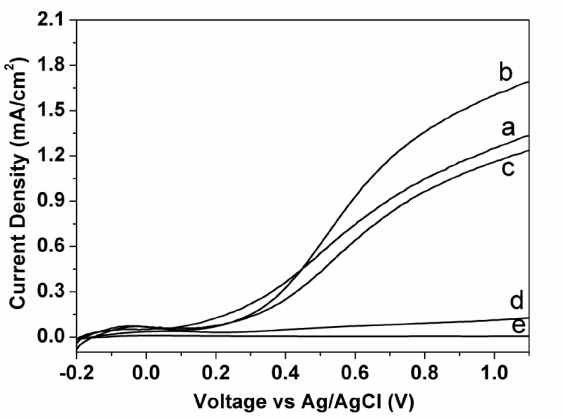

Fig. 5 Photocurrent curves of the W-doped $BiVO_4$ samples calcined at 500 ℃ for 30 min with different doping concentrations. a. 1 % W; b. 2 % W; c. 3 % W; pure $BiVO_4$ sample under light irradiation (d) and in dark (e)

photo-electrochemical property of W-doped $BiVO_4$ samples is investigated. The photocurrent curves of the W-doped $BiVO_4$ samples calcined at different temperatures are shown in Fig. 6. The result shows that the photocurrent obviously increases when the calcination temperature is increased from 450 to 550 ℃, which may be due to the improvement of the crystallization. While for the W-doped $BiVO_4$ sample calcined at 550 ℃, the photocurrent is lower than that calcined at 500 ℃. The decrease of photocurrent may be due to the easier recombination of photo-generated carriers induced by the relatively larger crystal size of the sample after calcination at higher temperature.

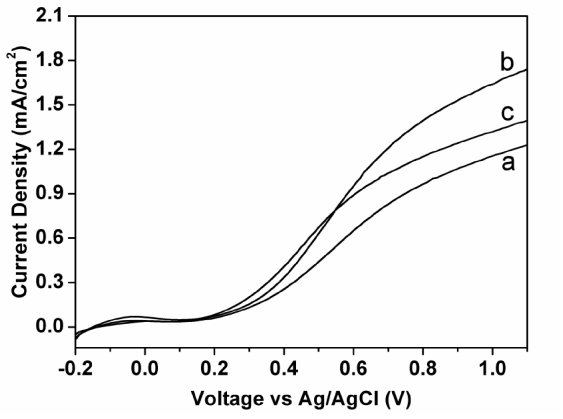

Fig. 6 Photocurrent curves of the $BiVO_4$ samples with 2 % W-doped and calcined at different calcination temperatures. a. 450 ℃; b. 500 ℃; c. 550 ℃ for 30 min

The influence of calcination time on the photo-electrochemical property of W-doped $BiVO_4$ samples is also investigated. Photocurrent curves of the $BiVO_4$ samples with 2 % W-doped and calcined at 500 ℃ for different time are shown in Fig. 7. When the calcination time is increased from 30 min to 2 h, the photocurrent obviously decreases. The crystal size of the $BiVO_4$ sample grows with the increase of calcination time, which may induce the easier recombination of photo-generated carriers. Thus, proper calcination temperature and time are crucial to obtain high photocurrent.

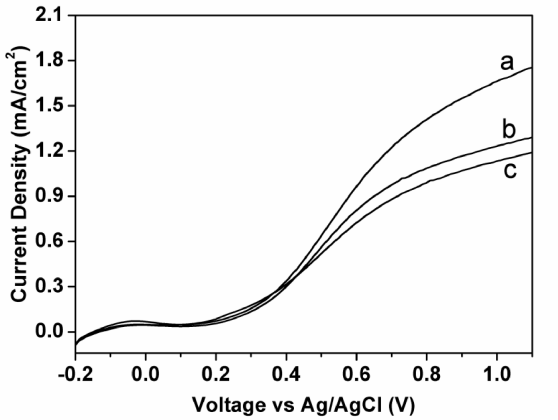

Fig. 7 Photocurrent curves of the $BiVO_4$ samples with 2 % W-doped and calcined at 500 ℃ for different time. a. 30 min; b. 1 h; c. 2 h

The photochemical stability of a photoelectrode is another crucial point for a photoelectrochemical cell. Since the photocurrent of the W-doped $BiVO_4$ can be enhanced after the surface pretreatment, the stability of the photocurrent after the surface pretreatment should be investigated for practical application. The photocurrent - time (i - t) curve of W-doped $BiVO_4$ after surface pretreatment in 0.5 M Na_2SO_4 aqueous solution is shown in Fig. 8. The photocurrent of W-doped $BiVO_4$ is initially about 0.95 mA · cm^2 and decreases to about 0.76 mA · cm^2 after 60 min of illumination. The photocurrent of W-doped $BiVO_4$ increases to 3 times after the pretreatment, while the photocurrent only deceases to 80 % in air after 60 min and still much higher than the photocurrent before the surface pretreatment. XRD of the W-doped $BiVO_4$ samples before and after illumination was also used to demonstrate

the photostability of the W-doped $BiVO_4$ photoanode in 0.5 M Na_2SO_4 aqueous solution (Fig. 9). Thus, the results suggest that the W-doped $BiVO_4$ photoanode after surface pretreatment is assumed to be stable in 0.5 M Na_2SO_4 aqueous solution for 60 min, and the photocurrent reduction during illumination may come from some oxidized species on the photoelectrode surface or extremely low surface corrosion [4].

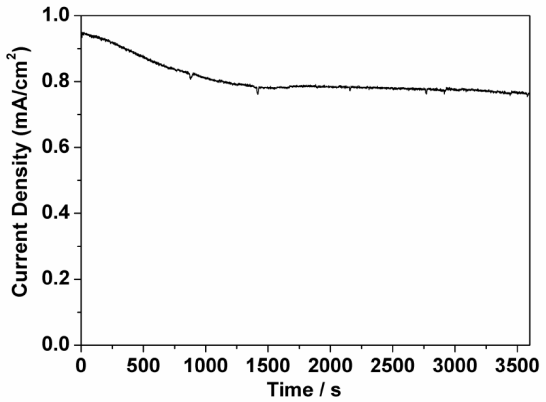

Fig. 8　Chronoamperometry (i - t) curve of 2 % W-doped $BiVO_4$ electrodes in a 0.5 M Na_2SO_4 aqueous solution (pH = 6.5); a AM 1.5 G sunlight simulator (Oriel 92251A-1000), a three-electrode system, the potential: 0.65 V vs. Ag/AgCl

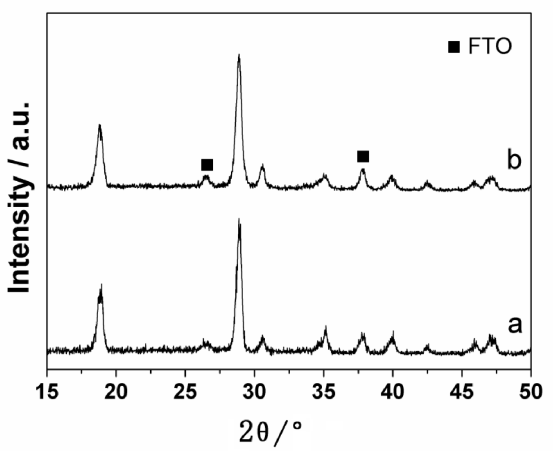

Fig. 9　XRD patterns of the W-doped $BiVO_4$ before (a) and after (b) illumination in a 0.5 M Na_2SO_4 aqueous solution, potential: 0.65 V vs. Ag/AgCl

4　Conclusions

In summary, W-doped $BiVO_4$ thin films were deposited by drop-casting method. The $BiVO_4$ thin films possessed a monoclinic structure. 2 % W-doped $BiVO_4$ sample calcined at 500 ℃ for 30 min after the electrochemical surface pretreatment showed the highest photoelectrochemical performance. Both tungsten doping and the electrochemical surface pretreatment can improve the photoelctrochemical response of the $BiVO_4$ thin films, which is attributed to the improvement of the conductivity and the separation of photo-generated carriers and the removal of surface recombination center.

References:

[1]　Zhou L L. Synthesis of BiOBr/I nanocomposites and photocatalytic activities to organic compounds [J]. J Sichuan Univ: Nat Sci Ed, 2015, 52: 370 (in Chinese).

[2]　Cesar I, Kay A, Gonzalez Martinez J A, *et al*. Translucent thin film Fe_2O_3 photoanodes for efficient water splitting by sunlight: Nanostructure-directing effect of Si-doping [J]. J Am Chem Soc, 2006, 128: 4582.

[3]　Santato C, Odziemkowski M, Ulmann M, *et al*. Crystallographically oriented mesoporous WO_3 films: synthesis, characterization, and applications [J]. J Am Chem Soc, 2001, 123: 10639.

[4]　Luo W J, Yang Z S, Li Z S, *et al*. Solar hydrogen generation from seawater with a modified $BiVO_4$ photoanode [J]. Energy Environ Sci, 2011, 4: 4046.

[5]　Long M C, Cai W M, Kisch H. Visible light induced photoelectrochemical properties of n-$BiVO_4$ and n-$BiVO_4$/p-Co_3O_4 [J]. J Phys Chem C, 2008, 112: 548.

[6]　Hong S J, Lee S, Jang J S, *et al*. Heterojunction $BiVO_4/WO_3$ electrodes for enhanced photoactivity of water oxidation [J]. Energy Environ Sci, 2011, 4: 1781.

[7]　Kudo A, Ueda K, Kato H, *et al*. Photocatalytic O_2 evolution under visible light irradiation on $BiVO_4$ in aqueous $AgNO_3$ solution [J]. Catal Lett, 1998, 53: 229.

[8]　Kudo A, Omori K, Kato H. A novel aqueous process for preparation of crystal form-controlled and highly crystalline $BiVO_4$ powder from layered vanadates at room temperature and its photocatalytic and photophysical properties [J]. J Am Chem Soc, 1999, 121: 11459.

[9] Luo H M, Mueller A H, McCleskey T M, *et al*. Structural and photoelectrochemical properties of $BiVO_4$ thin films [J]. J Phys Chem C, 2008, 112: 6099.

[10] Park H S, Kweon K E, Ye H, *et al*. Factors in the metal doping of $BiVO_4$ for improved photoelectrocatalytic activity as studied by scanning electrochemical microscopy and first-principles density-functional calculation [J]. J Phys Chem C, 2011, 115: 17870.

[11] Rao P M, Cai L L, Liu C, *et al*. Simultaneously efficient light absorption and charge separation in $WO_3/BiVO_4$ core/shell nanowire photoanode for photoelectrochemical water oxidation [J]. Nano Lett, 2014, 14: 1099.

[12] Li Z S, Luo W J, Zhang M L, *et al*. Photoelectrochemical cells for solar hydrogen production: current state of promising photoelectrodes, methods to improve their properties, and outlook [J]. Energy Environ Sci, 2013, 6: 347.

[13] Li M T, Zhao L, Guo L J. Preparation and photoelectrochemical study of $BiVO_4$ thin films deposited by ultrasonic spray pyrolysis [J]. Int J Hydrogem Energ, 2010, 35: 7127.

[14] Sayama K, Nomura A, Arai T, *et al*. Photoelectrochemical decomposition of water into H_2 and O_2 on porous $BiVO_4$ thin-film electrodes under visible light and significant effect of Ag ion treatment [J]. J Phys Chem B, 2006, 110: 11352.

[15] Su J, Guo L, Yoriya S, *et al*. Aqueous growth of pyramidal-shaped $BiVO_4$ nanowire arrays and structural characterization: application to photoelectrochemical water splitting [J]. Cryst Growth Des, 2010, 10: 856.

[16] Ng Y H, Iwase A, Kudo A, *et al*. Reducing graphene oxide on a visible-light $BiVO_4$ photocatalyst for an enhanced photoelectrochemical water splitting [J]. J Phys Chem Lett, 2010, 1: 2607.

[17] Seabold J A, Choi K S. Efficient and stable photooxidation of water by a bismuth vanadate photoanode coupled with an iron oxyhydroxide oxygen evolution catalyst [J]. J Am Chem Soc, 2012, 134: 2186.

[18] Berglund S P, Flaherty D W, Hahn N T, *et al*. Photoelectrochemical oxidation of water using nanostructured $BiVO_4$ films [J]. J Phys Chem C, 2011, 115: 3794.

[19] Park H S, Kweon K E, Ye H, *et al*. Factors in the metal doping of $BiVO_4$ for improved photoelectrocatalytic activity as studied by scanning electrochemical microscopy and first-principles density-functional calculation [J]. J Phys Chem C, 2011, 115: 17870.

[20] Ye H, Park H S, Bard A J. Screening of electrocatalysts for photoelectrochemical water oxidation on W-doped $BiVO_4$ photocatalysts by scanning electrochemical microscopy [J]. J Phys Chem C, 2011, 115: 12464.

[21] Zhong D K, Choi S, Gamelin D R. Near-complete suppression of surface pecombination in solar photoelectrolysis by "Co-Pi" catalyst-modified W:$BiVO_4$ [J]. J Am Chem Soc, 2011, 133: 18370.

[22] Luo W J, Li Z S, Yu T, *et al*. Effects of surface electrochemical pretreatment on the photoelectrochemical performance of Mo-doped $BiVO_4$ [J]. J Phys Chem C, 2012, 116: 5076.

[23] Pattengale B, Ludwig J, Huang J. Atomic insight into the W-doping effect on carrier dynamics and photoelectrochemical properties of $BiVO_4$ photoanodes [J]. J Phys Chem C, 2016, 120: 1421.

[24] Corbel G, Laligant Y, Goutenoire F, *et al*. Effects of partial substitution of Mo^{6+} by Cr^{6+} and W^{6+} on the crystal structure of the fast oxide-ion conductor structural effects of W^{6+} [J]. Chem Mater, 2005, 17: 4678.

[25] Karakitsou K E, Verykios X E. Effects of altervalent cation, doping of TiO_2 on its performance as a photocatalyst for water cleavage [J]. J Phys Chem, 1993, 97: 1184.